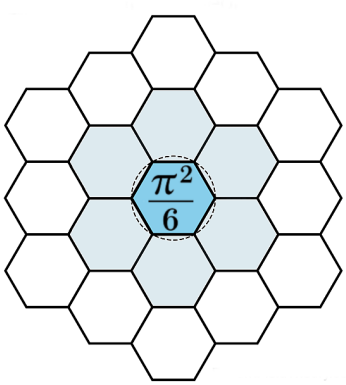

Basel constant $\pi^2/6$ on the central hexagon (AOL).

Surface Tension, Dipolar Repulsion, and Spatial Symmetry Breaking on the Allen Orbital Lattice (AOL)

James Johan Sebastian Allen

PatternFieldTheory.com
November 2025

Abstract

Ferrofluid labyrinths in Hele–Shaw cells are a canonical instance of pattern selection under competition between interfacial tension and long-range magnetostatic repulsion. We formulate this mechanism on the *Allen Orbital Lattice* (AOL), a hexagonal discrete substrate for nonlocal gradient flows, and derive a conservative dynamics for a nodewise volume fraction ϕ. The model is a lattice analogue of a nonlocal Cahn–Hilliard/Ohta–Kawasaki functional, with hex-stencil curvature and a dipolar kernel. We analyze mode competition and wavelength selection on the AOL via discrete Fourier symbols and show how control of lattice couplings yields the observed fingering-to-labyrinth transition. We place the framework in the context of post-1998 developments: room-temperature skyrmion lattices in 2D magnets, photonic Ising machines, and neutral-atom mega-arrays (6,100 qubits), arguing these platforms constitute physical or computational realizations of AOL-style energy minimization. The AOL provides a unifying discretization that is symmetry-consistent, spectrally well-conditioned, and experimentally proximate to emerging hardware.

1 Introduction

Labyrinthine microstructures arise in diverse media where a local interfacial penalty competes against a nonlocal repulsion. Early continuum analyses of ferrofluid labyrinths in Hele–Shaw cells emphasized overdamped gradient flows of a volume fraction field governed by surface tension and magnetostatics. On a discrete substrate, symmetry and stencil choice strongly affect curvature, anisotropy leakage, and the selected length scales. The *Allen Orbital Lattice* (AOL) is a hexagonal tiling we adopt as the natural discrete plane for such processes: its sixfold symmetry minimizes grid artifacts and aligns with numerous crystalline, magnetic, and moiré contexts.

This paper develops an AOL-based model for ferrofluid labyrinths, derives its conservative gradient flow, and presents a spectral selection picture that unifies ferrohydrodynamic fingering, nonlocal phase separation, and modern lattice realizations (skyrmion crystals, photonic/neutral-atom Ising solvers, and moiré flat-band systems) [1, 2, 3, 4, 5, 7, 9, 10, 11].

2 Continuum background (brief)

Let $\phi(x,t) \in [0,1]$ denote the coarse-grained volume fraction of magnetic fluid in a thin gap domain $\Omega \subset \mathbb{R}^2$. A standard energy is

$$\mathcal{F}[\phi] = \int_\Omega \left(\tfrac{\gamma}{2} |\nabla \phi|^2 + \beta W(\phi) \right) dx + \frac{\alpha}{2} \iint_{\Omega\times\Omega} K(x-y)(\phi(x)-\bar{\phi})(\phi(y)-\bar{\phi})\, dx\, dy, \tag{1}$$

with interfacial weight $\gamma > 0$, double-well $W(\phi) = \phi^2(1-\phi)^2$, mean $\bar{\phi} = \frac{1}{|\Omega|}\int \phi$, and dipolar kernel K. With conserved dynamics,

$$\partial_t \phi = \nabla \cdot (M \nabla \mu), \qquad \mu = \frac{\delta \mathcal{F}}{\delta \phi} = -\gamma \Delta \phi + \beta W'(\phi) + \alpha (K * (\phi - \bar{\phi})). \tag{2}$$

This captures the labyrinth selection as a competition between the stabilizing $-\gamma\Delta\phi$ and the destabilizing nonlocal term.

3 AOL discretization

We place nodes $i = 1, \ldots, N$ on a hexagonal lattice (spacing h) with six-neighbor set $\mathcal{N}(i)$. The state variable is $\phi_i \in [0,1]$, with conserved sum $\sum_i \phi_i = \Phi_0$. Define the lattice free energy

$$\mathcal{F}_d(\phi) = \gamma \sum_{\langle i,j \rangle} w_{ij} (\phi_i - \phi_j)^2 + \frac{\alpha}{2} \sum_{i,j} K_{ij} (\phi_i - \bar{\phi})(\phi_j - \bar{\phi}) + \beta \sum_i W(\phi_i), \tag{3}$$

where $w_{ij} > 0$ are hex-stencil weights (e.g., $w_{ij} = \frac{1}{2h^2}$), $\bar{\phi} = \frac{1}{N}\sum_i \phi_i$, and $K_{ij} = K(r_{ij})$ with r_{ij} the planar distance; for thin films, $K(r) \sim r^{-3}$ with short-range regularization.

Lattice chemical potential.

$$\mu_i = \frac{\partial \mathcal{F}_d}{\partial \phi_i} = 2\gamma \sum_{j \in \mathcal{N}(i)} w_{ij}(\phi_i - \phi_j) + \alpha \sum_j K_{ij}(\phi_j - \bar{\phi}) + \beta W'(\phi_i). \tag{4}$$

Conserved gradient flow. Let ∇_d and div_d be the hex-gradient/divergence. With constant mobility M,

$$\partial_t \phi_i = \mathrm{div}_d (M\, \nabla_d \mu)_i\,. \tag{5}$$

Equations (4)–(5) define the AOL dynamics. Mass is conserved and $\mathcal{F}_d$ is nonincreasing.

4 Linear stability and pattern selection

Linearize $\phi_i = \bar{\phi} + u_i$ with small u. On a periodic hex lattice, mode k has discrete symbol $\hat{L}(k) = 2\gamma\,\hat{\Delta}_{\mathrm{hex}}(k) + \alpha\,\hat{K}(k) + \beta W''(\bar{\phi})$, where $\hat{\Delta}_{\mathrm{hex}}$ is the Fourier symbol of the hex Laplacian and $\hat{K}$ is the discrete Fourier transform of K_{ij}. The growth rate for conserved dynamics is $\sigma(k) = -M|\hat{\nabla}(k)|^2\hat{L}(k)$. Instability requires $\hat{L}(k) < 0$, selecting a band of wavenumbers; the fastest-growing k_* sets the labyrinth spacing. Compared to square grids, the hex symbol suppresses spurious anisotropy, yielding cleaner ring-like power spectra and more isotropic labyrinths at equal resolution.

5 Numerics

A semi-implicit convex–concave split treats the γ-Laplacian and convex part of W implicitly and the nonlocal convolution explicitly. For speed, embed the hex grid in a skewed rectangular array and use FFT-based convolution for K_{ij} with periodic boundaries; otherwise truncate K beyond a few spacings without significant change in selected k_*. Initialization with a perturbed droplet and a field ramp in α reproduces fingering, coarsening arrest, and stationary labyrinths.

6 Parameter interpretation

Interfacial tension γ sets interface thickness and penalizes curvature; **nonlocal weight** α encodes field/magnetization strength; **mean fraction** $\bar{\phi}$ fixes coverage; **mobility** M sets time units. Weak noise seeds the fingering wavelength; quenches in α or γ change k_* predictably via $\hat{L}(k)$.

7 Related platforms (post-1998) and AOL unification

7.1 Skyrmion and chiral spin textures

Room-temperature skyrmion lattices in layered 2D magnets (e.g., Fe_3GaTe_2) have been observed at zero field and high density [2, 3, 4]. Their microstructure energy (exchange, DMI, anisotropy, Zeeman, dipolar) maps to an AOL nonlocal functional with additional chiral gradient terms. The labyrinth–stripe–bubble triad in thin films is a close analogue of our γ vs. α competition.

7.2 Photonic Ising machines

All-to-all and large-N photonic Ising platforms now solve dense spin Hamiltonians with programmable couplings, including free-space MZI implementations and OEO time-multiplexed loops reaching $\sim$200 GOPS and very large spin counts [6, 7, 5]. These can minimize discretized AOL energies ($\{\phi_i\} \in \{0, 1\}$ or ± 1), providing hardware acceleration for pattern selection and kernel exploration.

7.3 Neutral-atom mega-arrays

Optical tweezer arrays with 6,100 coherent neutral-atom qubits and 12.6-s coherence times [9, 8] furnish a physical, reconfigurable lattice with native hex/kagomé geometries and tunable nonlocal gates. AOL kernels can be emulated by Rydberg-mediated interactions or graph-coupling schedules, enabling laboratory exploration of our dispersion predictions at scale.

7.4 Twistronics, flat bands, super-moiré

Twisted multilayers generate tunable moiré superlattices with flat bands and unconventional superconductivity/topology [10, 11, 12, 13, 14, **?**]. The moiré-controlled interaction range and band geometry correspond to AOL kernel shaping: by modulating $\hat{K}(k)$, one steers the unstable band and thus the labyrinth spacing.

8 Implications and outlook

The AOL furnishes a symmetry-respecting discrete plane for nonlocal gradient flows that (i) matches ferrofluid labyrinth phenomenology, (ii) aligns with magnetic microstructure energetics, and (iii) plugs into contemporary lattice hardware. Immediate directions include: calibrated kernel recovery from experiments; photonic/neutral-atom emulation of $\hat{K}(k)$ families; and AOL-based dispersion engineering for target wavelengths in soft matter and spintronics.

Methods (discrete symbols on the hex lattice)

On a hex tiling with primitive vectors a_1, a_2 and reciprocal basis b_1, b_2, the 6-neighbor Laplacian has symbol

$$\hat{\Delta}_{\text{hex}}(k) = \frac{2}{h^2}[\cos(k\cdot a_1) + \cos(k\cdot a_2) + \cos(k\cdot(a_1 - a_2)) - 3]\,.$$

For an isotropic $K(r)$, $\hat{K}(k)$ is radial and evaluated via discrete Hankel/FFT on the embedded skew grid. The fastest-growing ring k_* solves $\partial_k \hat{L}(k) = 0$ with $\hat{L}(k_*) < 0$.

Simulation protocol (for reproduction)

Grid: 512×512 hex-embedded; spacing $h = 1$. Parameters: $\gamma \in [0.5, 2]$, $\alpha \in [0, 20]$, $\beta = 1$, $M = 1$; time step $\Delta t = 0.1$ (semi-implicit). Start from a radius-R droplet with 1% boundary noise; ramp α from 0 to target over 200 steps; run to $T = 5\times10^3$. Output: ϕ, spectrum $|\hat{\phi}(k)|^2$, k_*, interface length.

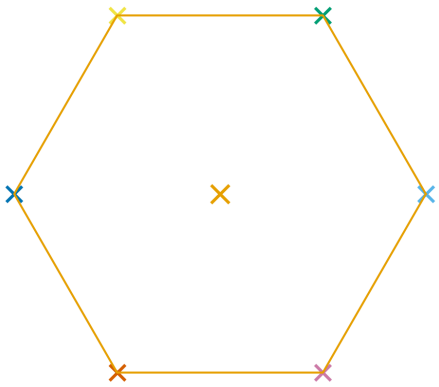

Figure 1: (Top) AOL hexagonal neighbor stencil. Sixfold rotational symmetry suppresses anisotropy leakage and yields curvature estimates consistent with isotropic continuum limits. (Bottom) Labyrinthine microstructure (ϕ) under increasing α at fixed γ on the AOL substrate. The selected wavelength matches the fastest-growing ring mode k_* predicted by the discrete hex-symbol analysis.

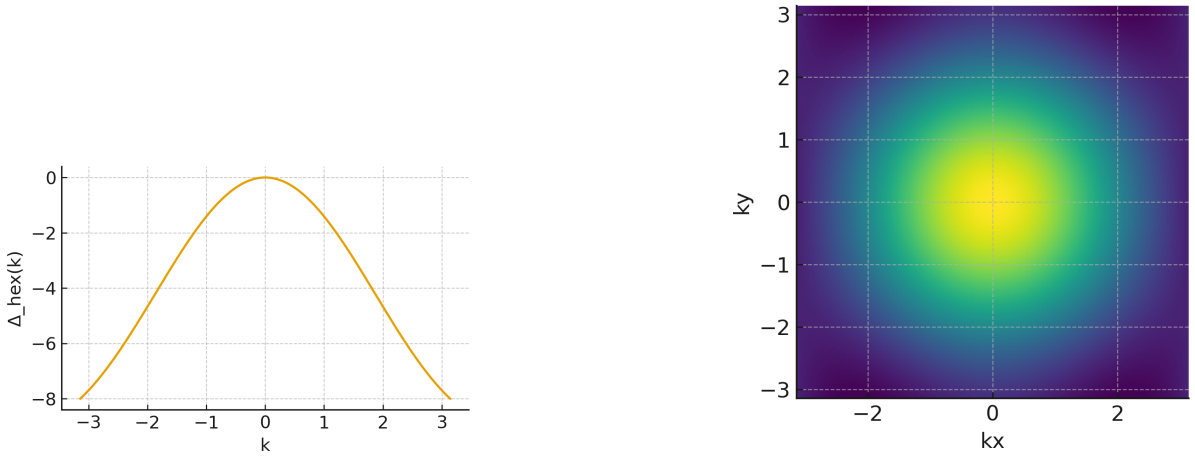

Figure 2: Dispersion $\sigma(k)$ on the AOL. Left: radial band structure indicating the fastest-growing mode k_*. Right: full 2D $\sigma(k)$ showing isotropic instability bands from the hexagonal stencil.

Conclusion

By placing ferrofluid labyrinth dynamics on the Allen Orbital Lattice we obtain a compact, symmetry-faithful, and hardware-adjacent formulation of nonlocal pattern selection. The same lattice viewpoint connects naturally to skyrmion microstructures, photonic Ising machines, neutral-atom arrays, and moiré superconductors, suggesting a common language for designing—and physically realizing—target patterns via kernel shaping on hexagonal lattices.

Data and code. Reference implementation (hex-embedded FFT, semi-implicit stepper) available upon request; figures can be regenerated with the protocol above.

References

[1] F. Otto, *Evolution of Microstructures: An Example*, Arch. Rational Mech. Anal. **141**, 63–103 (1998).

[2] C. Zhang *et al.*, *Above-room-temperature chiral skyrmion lattice at zero magnetic field in* $Fe_{3-x}GaTe_2$, Nat. Commun. **15**, 48799 (2024).

[3] Z. Zhang *et al.*, *Topological Magnetism: Materials and Devices*, Adv. Funct. Mater. (2025).

[4] Y. Zhang *et al.*, *Stable skyrmion bundles at room temperature and zero field*, Nat. Commun. **15**, 47730 (2024).

[5] J. Ouyang *et al.*, *On-demand photonic Ising machine with simplified Hamiltonian*, Commun. Phys. **7**, 01658 (2024).

[6] J. Wang *et al.*, *All-to-All Connected Photonic Ising Machine with Arbitrary Couplings*, CLEO 2024 (Optica).

[7] Z. Zhang *et al.*, *Programmable Hopfield-inspired photonic Ising machine at 200 GOPS*, arXiv:2509.09581 (2025).

[8] H. J. Manetsch *et al.*, *A tweezer array with 6100 highly coherent atomic qubits*, arXiv:2403.12021 (2024).

[9] H. J. Manetsch *et al.*, *A tweezer array with 6100 highly coherent atomic qubits*, Nature **626**, 9641 (2025).

[10] D. Zhai *et al.*, *Twistronics and moiré superlattice physics in 2D TMDs*, Rep. Prog. Phys. **88**, 084501 (2025).

[11] Q. Deng *et al.*, *Ultraflat bands in twisted moiré superlattices under shallow potentials*, Phys. Rev. B **111**, 155145 (2025).

[12] M. R. Koblischka *et al.*, *Review of moiré superconductivity*, Mater. Today Phys. **38**, 100793 (2024).

[13] S. Liu *et al.*, *Three-dimensional flat bands and possible interlayer triplet pairing in alternating-twisted* $NbSe_2$ *moiré bulk*, arXiv:2509.09109 (2025).

[14] C.-K. Chiu *et al.*, *Double and quadruple flat bands tuned by alternating magnetic fluxes in tBLG*, Phys. Rev. Lett. **132**, 246401 (2024).

Document Timestamp and Provenance

This document is part of Pattern Field Theory (PFT) and Allen Orbital Lattice (AOL). Public timestamps, server logs, archival snapshots, hash signatures, and notebooks (since **May 2025**) establish authorship continuity and priority.

`patternfieldtheory.com`